Key Engineering Materials
ISSN: 1662-9795, Vol. 926, pp 452-459
doi:10.4028/p-y37nm3

Submitted: 2021-12-09
Revised: 2022-02-28
Accepted: 2022-02-28
Online: 2022-07-22

FEM Analysis of the Skin Contamination Behavior in the Extrusion of a AA6082 Profile

Marco Negozio[1,a*], Riccardo Pelaccia[2,b], Lorenzo Donati[1,c] and Barbara Reggiani[2,d]

[1*]DIN- Department of Industrial Engineering, University of Bologna, Viale Risorgimento 2, 40136, Bologna, Italy

[2]DISMI- Department of Sciences of Methods for Engineering, University of Modena and Reggio Emilia, Viale Amendola 2, 42124, Reggio Emilia, Italy

[a]marco.negozio2@unibo.it, [b]riccardo.pelaccia@unimore.it, [c]l.donati@unibo.it, [d]barbara.reggiani@unimore.it

Keywords: skin contamination, back-end defect, FEM, Qform, extrusion

Abstract. In the extrusion of aluminum alloys, the skin contamination lead to the scraping of the profile extent in which this defect occurs. In order to optimize the scraping process, extrusion companies and die makers can either perform time-consuming and expensive analyses to experimentally determine the evolution of the defect or rely on predictive methods. Recently, numerical methods, as the Finite Elements, are increasingly used to predict the evolution of the skin contamination, but their accuracy is still uncertain. In this work, an AA6082 aluminum profile of industrial complexity is analysed and the data collected used to validate an innovative method for the prediction of the skin contamination evolution developed using the commercial FEM code Qform®. In addition, the results are used to assess the prediction accuracy of an industrial empirical formula often used by operators.

Introduction

The extrusion of Al-Mg-Si aluminum alloys represents a competitive manufacturing solution to produce profiles with complex geometries and constant cross sections. These profiles are used in sectors such as civil, industrial and automotive due to several properties, which make these alloys particularly suitable for these markets [1-4]. For structural applications, mechanical properties must be consistent throughout the extent of the profile, so that defects deteriorating such properties cannot be tolerated.

In particular, the billet skin contamination, also known as back-end defect since occurring at the end of each extruded billet, may compromise mechanical properties [5] and lead to the scraping of material. This defect is related to the outer surface (also called skin) of the billet marked by different properties than those of the inner material, as microstructure and chemical composition. These differences are caused by the manufacturing process of the billet (DC-casting) and by the presence of impurities such as oxides, lubricant or dust that adhere to the external layer of the billet during several stages before the extrusion [1]. As shown in Fig. 1, during the process stroke, the skin volume (red in the figure) accumulates near the ram in relation to the high friction factor with the container and, as the former advances, it flows towards the centre of the billet and the extrusion die. In order to avoid the defect contamination, the most important parameter to fix is the length of the billet rest, that must be optimized to prevent the skin from flowing into the die space and, consequently, into the profile (Fig. 1d). The defect contamination starts at the end of an extrusion (negative distance with respect to stop-mark, which is a clearly visible mark on the profile surface generated by the adhesion of the material on the bearing zone in the billet replacement [6, 7]) and ends on charge welds at positive values after the stop-mark.

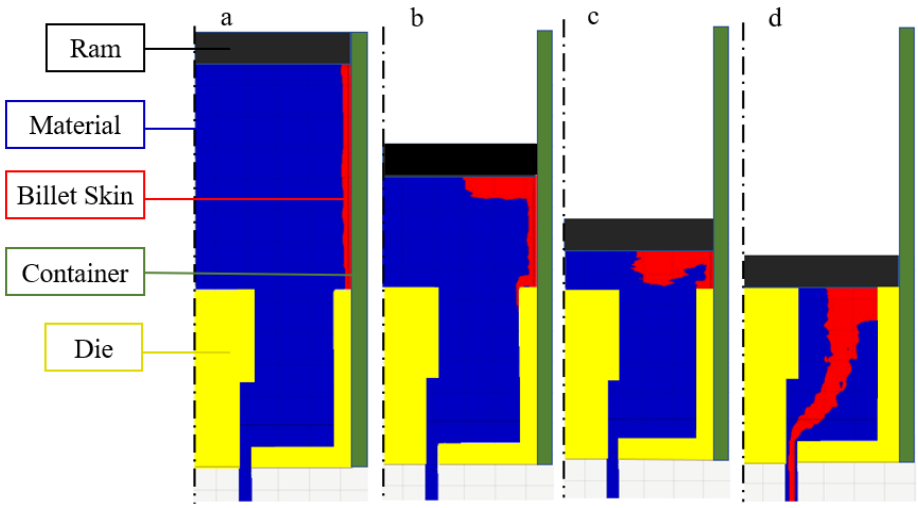

Figure 1: Schematic explanation of the billet skin behaviour during forward extrusion.

The behaviour of the skin defect was studied mostly by experiments: Finkelnburg WD et al. [8], Kim YT et al. [1] and Jowett C et al. [9] studied the billet surface flow to quantify the effect of the process parameters on the inflow of billet skin. Ishikawa T et al. [14] and Hatzenbichler T et al. [10] investigated the prediction of the skin flow on extruded profiles with a simple symmetrical geometry. Only two studies were performed to investigate the skin defect on profiles of industrial complexity: Lou S et al. [11] for a hollow profile, Negozio et al. [12] for two solid profiles. Both of these studies show that some further efforts have to be made in order to improve the precision of the FEM codes to better predict the behaviour of the skin contamination.

To the best author's knowledge, only one empirical formula (1) has been reported in the literature by Jowett et al. [10] for skin contamination prediction:

$$s = \frac{(14\% \times Vb - 75\% \times (V1 + V2) - Vrest)}{Ae \times n} \quad (1)$$

where *Vb* and *Vrest* are the billet and the billet rest volumes, respectively, *V1* the volume of material in the die ports, *V2* the volume of material in the welding chambers, *Ae* the exit profile section area and *n* the number of profile openings in the die.

In this context, the aim of this work was to investigate the simulation accuracy on the skin contamination prediction by comparing the experimental results on a AA6082 extruded industrial profile with the numerical outputs achieved with the Qform® code and the outcome of the empirical formulae available in the literature.

Experimental Procedure

The experimental analysis of the examined profile is reported in detail in Negozio et al. [13], where an in-depth investigation on the evolution of the skin contamination defect was carried out. In Fig. 2 is reported the geometry of the profile while Fig. 3 shows the skin evolution as percentage of the profile cross-sectional area over the distance from the stop mark with two image analyses.

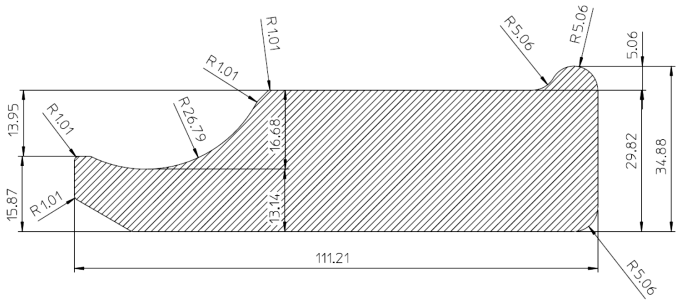

Figure 2: Profile under investigation.

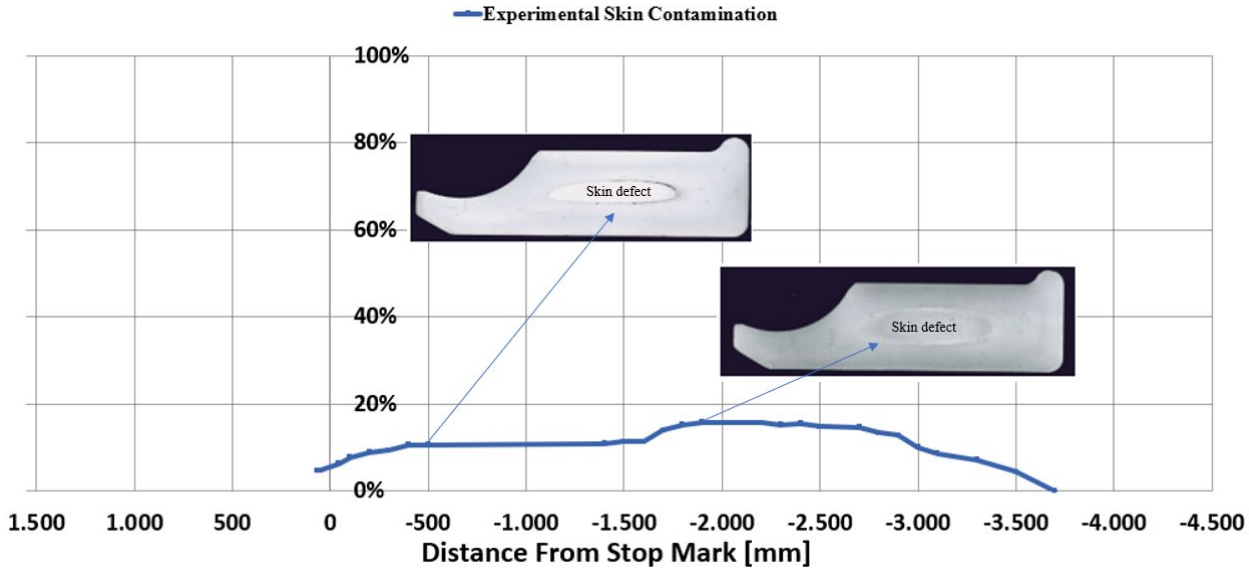

Figure 3: Skin contamination evolution over the stop mark distance.

As depicted by Fig. 3, where negative values on x-axis represent samples extracted from the end of the extrusion of the previous billet, the value "0" represent the stop-mark and the positive ones represent samples extracted from the start of the extrusion of the new billet, the skin contamination appears at -3750 mm from the stop mark, it enlarges up to a certain value (15-20%) and remains nearly constant for the remaining stroke, until it disappears around the stop mark point, where the billet material replacement (charge welds) takes place. These experimental data will be compared with the numerical and analytical predictions in order to assess their accuracy.

Table 1: Process parameters and geometry tolerances.

Process Parameter	
Aluminum alloy	AA6082
Ram speed [mm/s]	7.64
Container temperature [°C]	440
Billet temperature [°C]	530
Die temperature [°C]	450
Ram acceleration time [s]	5
Extrusion ratio	20
Billet length [mm]	990
Billet diameter [mm]	254
Container diameter [mm]	266
Billet Rest length [mm]	15
Skin thickness [μm]	250

In Tab. 1, the material and process parameters are summarized.

Numerical Investigation

Numerical simulations were performed by using the Lagrangian FEM code Qform®. Starting from the CAD files of the tools and billet, the mesh was generated using the Qform® internal tool Qshape, which allows the preparation of the volumetric meshes of the process components. The mesh details are summarized in Tab. 2.

Table 2: Mesh parameters.

Object	Nodes on surface	Internal nodes	Total nodes	Surface elements	Volumetric elements
Workpiece	5101	13715	18816	10198	99701
Ram	236	0	236	468	629
Container	2106	3	2109	4212	6305
Die	13698	11933	25631	27396	114630
Total	21141	25651	46792	42274	221265

The Hensel-Spittel law [14] was used to model the flow stress behaviour of the billet material:

$$\bar{\sigma} = A \cdot e^{m_1 T} \cdot \bar{\varepsilon}^{-m_2} \cdot \dot{\bar{\varepsilon}}^{-m_3} \cdot e^{\frac{m_4}{\bar{\varepsilon}}} \cdot (1+\bar{\varepsilon})^{m_5 T} \cdot e^{m_7 \bar{\varepsilon}} \cdot \dot{\bar{\varepsilon}}^{m_8 T} \cdot T^{m_9} \quad (2)$$

where $\bar{\sigma}$ is the flow stress, $\bar{\varepsilon}$ the strain, $\dot{\bar{\varepsilon}}$ the strain rate, T the temperature (°K) and A, m_1-m_9 material coefficients, reported in Tab. 3 for the investigated AA6082 alloy. These values were taken from the Qform material database.

Table 3: The Hensel-Spittel AA6082 coefficients.

Material parameters	AA6082
A	270 [MPa]
m1	-0.0045 [K^{-1}]
m2	-0.127
m3	0.13
m4	-0.016
m5	0.00026 [K^{-1}]
m7	0
m8	0 [K^{-1}]
m9	0

The other physical and thermal properties of the workpiece were set according to the values of the Qform® database for the AA6082 alloy.

Also concerning the tools (die, ram and container), the mechanical, physical and thermal parameters were set according to the default values of the H13 steel in the Qform® database.

In order to simulate the skin contamination behaviour, a number of tracked points were set on the billet part nearby the ram at a distance of 250 μm from the external surface (Fig. 4), as the skin contamination thickness was experimentally found of 250 μm (Tab. 1). After simulated the extrusion of the billet, Qform® allows a post-processing operation of point tracking to check the flow of the set points.

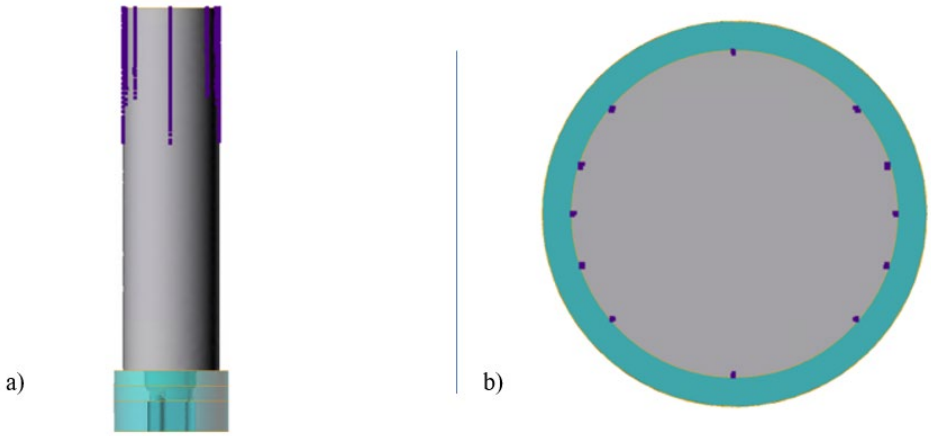

Figure 4: Selected tracking points (extrusion direction top-down): a) longitudinal view (the container is hided); b) transversal view.

The friction parameters are summarized in Tab. 4: a sticking condition was set for the billet-container surface as well as for the billet-die surface [15], a sliding condition with the Levanov friction law was set for the bearing surface (in accordance with what suggested from the friction Qform database) and a sliding condition with Levanov friction law was set for the billet-ram surface. Even if the maximum admissible value for the friction factor is 1 [16, 17], which correspond to the unlubricated condition, a value of 2 was set in the Levanov model for the billet-ram surface as the result of a performed sensitivity analysis. In Fig. 5, the point tracking behaviour of the extrusions with a billet-ram friction condition of 1 (Fig. 5a,c) and 2 (Fig. 5b,d) is reported: as it can be seen, when a) the points slide through the ram surface, while b) the points do not slide but flow through the inner part of the billet in the extrusion direction, in accordance with what is reported in the literature [6].

Table 4: Friction conditions.

Surface	Friction condition
Billet-Container	Sticking condition
Billet-Ram	Levanov model (m = 2, n = 1.25)
Billet-Die	Sticking condition
Bearings	Levanov model (m = 0.3, n = 1.25)

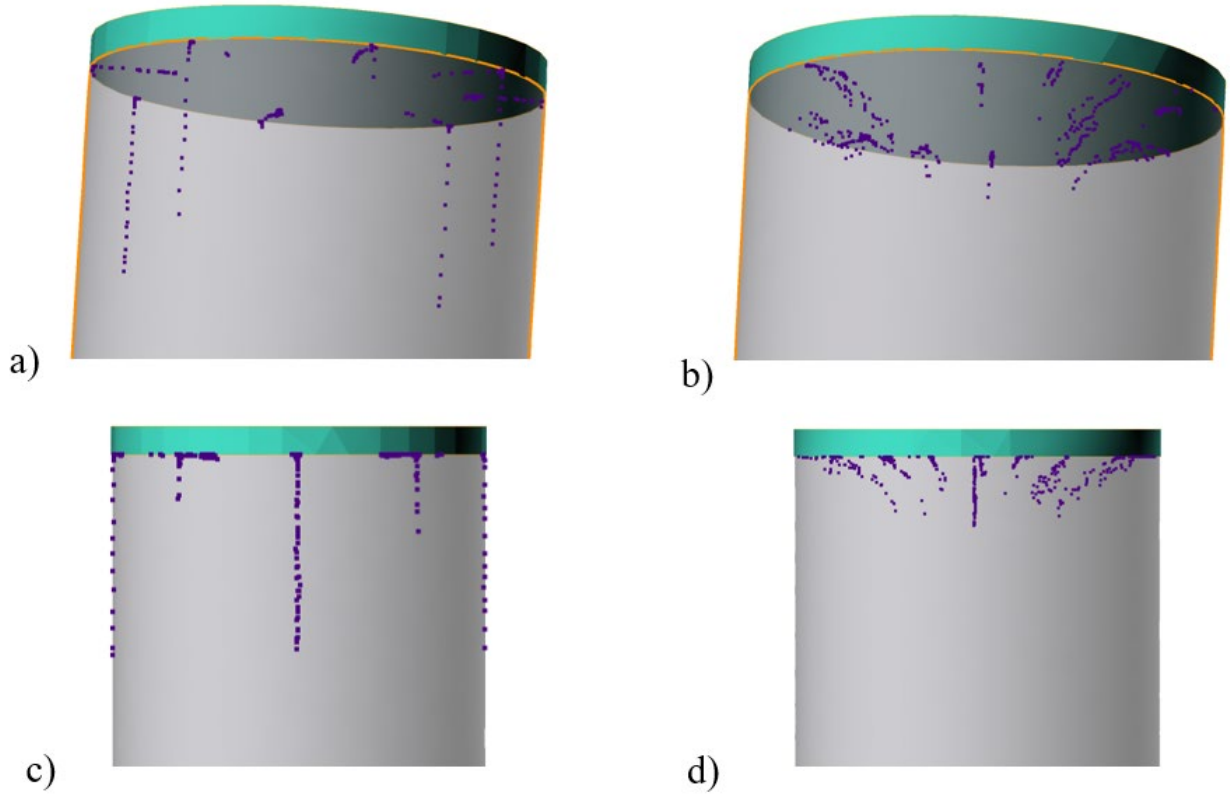

Figure 5: Skin points behaviour with a billet-ram friction factor value of a,c) 1 and b,d) 2.

Results and Discussion

In Fig. 6 is reported the main outcome of the performed numerical simulations with the point tracking highlighting the skin behaviour for three subsequent time steps.

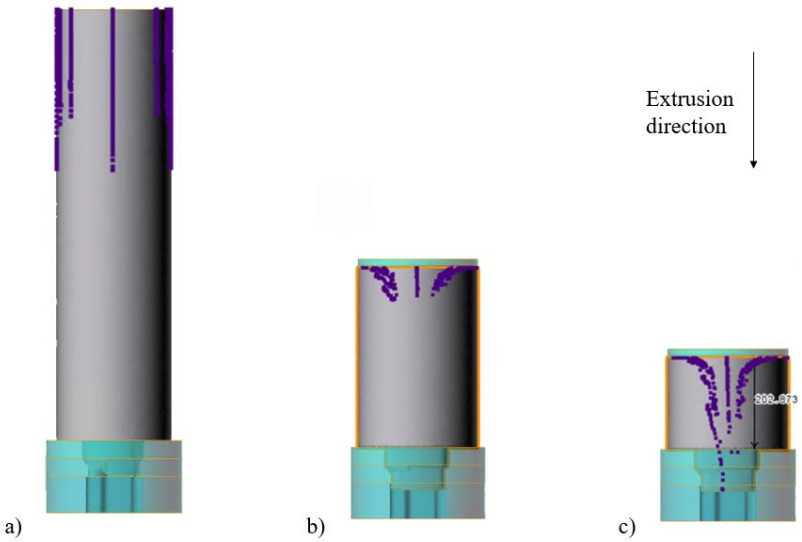

Figure 6: Point tracking operation at three simulation steps: a) start of the extrusion; b) half stroke; c) stroke at which the skin points started to flow into the bearings.

The exact ram-die distance where the skin points started to flow into the bearings zone was 202.8 mm (Fig. 6c) which means, considering the billet rest of 15 mm and the extrusion ratio of 20, that the predicted extent of the skin defect was 3756 mm. Compared to the experimental value of 3750 mm, an error of just 6 mm was found, thus proving the reliability of the predictive methodology.

In Fig. 7a,b, the comparison between the experimental and numerical shape of the defect in the cross section of the profile is shown. In Fig. 7c, it can be seen the image overlay of 7a and 7b: the figure furthermore proves the good matching between the experimental defect (in yellow) and the zone where the points are flowing in the simulation.

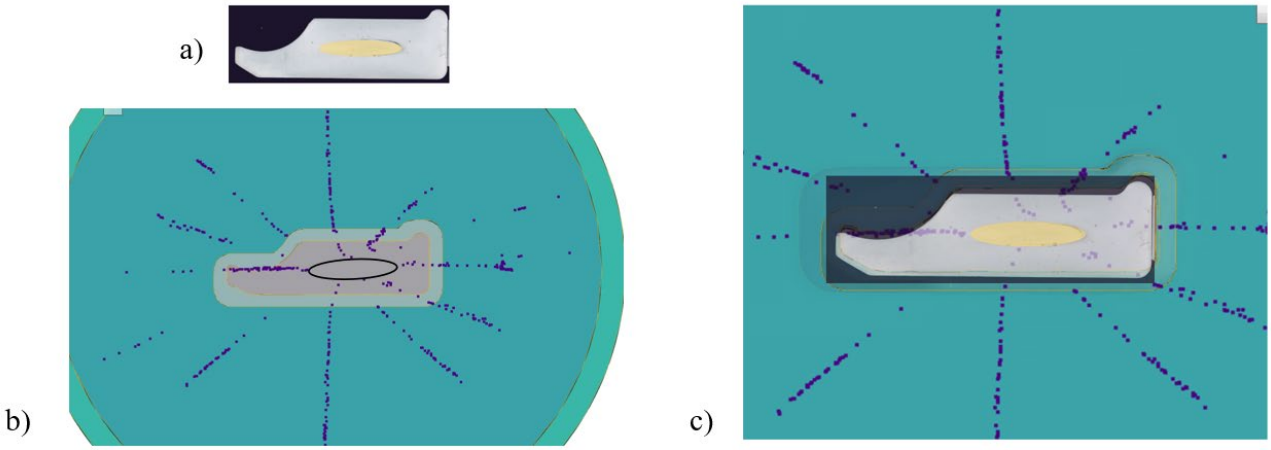

Figure 7: a) Experimental shape of the defect; b) numerical shape of the defect; c) comparison between numerical and experimental by image overlay.

The work proves the accuracy of the Lagrangian simulation for the skin tracking of the industrial profile. The main issue of the methodology is the computational time, which can be very long for profiles with complex geometries and for multi-holes dies, as those of industrial interest.

As reported in the introduction, experimental and numerical results were also compared to the defect extent predicted by the analytical formula of eqn. (1). As reported in Tab. 5, the formula accuracy is considerably less than that of the numerical one, leading to an error of 1595 mm (42.5%) of the defect extent.

Table 5: Comparison between experimental, numerical and obtained by the application of (1) results.

Method	Skin extents (distance from the stop mark)
Experimental	3750 mm
Numerical	3756 mm
Analytical (eqn. (1))	2155 mm

Conclusions

In the present work, a Lagrangian simulation using the commercial Qform® FEM code, together with the skin point tracking tool, was carried out for the evaluation of the skin defect extent on a solid extruded profile made with a AA6082 aluminium alloy previously experimentally tested by the same authors. The accuracy of the simulation was evaluated by the comparison of the predicted results with the experimental data and with the outcome of the analytical formula available in the literature. The main achievements of the work can be summarized as follows:

- An innovative method for the skin contamination prediction in the extrusion process was presented and discussed.
- A good matching was found between the numerical prediction and the experimental data of the skin contamination extent (numerical error below the 1%).
- A comparison between the result of the analytical formula and of the numerical investigation was made, proving the higher accuracy of the latter (the analytical error was 42.5%, the numerical below the 1%).

References

[1]. Y.T. Kim, K. Ikeda, Flow behavior of the billet surface layer in porthole die extrusion of aluminum, Metall Mater Trans A 31. (2000) 1635–1643.

[2]. N. Hashimoto, Application of Aluminum Extrusions to Automotive Parts. 150. (2015).

[3]. N. Parson, J. Fourmann, J.F. Beland, Aluminum Extrusions for Automotive Crash Applications, SAE Technical Papers. (2017) 1–16.

[4]. J. Hirsch, Automotive trends in aluminium - The European perspective, Materials Forum. 28(3) (2004) 15–23.

[5]. H. Valberg, M. Lefstad, A. Costa, On the Mechanism of Formation of Back-End Defects in the Extrusion Process, Procedia Manufacturing 47 (2020) 245-252.

[6]. B. Reggiani, T. Pinter, L. Donati, Scrap assessment in direct extrusion. Int J Adv Manuf Technol 107 (2020) 2635–2647.

[7]. M. Negozio, R. Pelaccia, L. Donati, B. Reggiani, T. Pinter, L. Tomesani, Finite Element Model Prediction of Charge Weld Behaviour in AA6082 and AA6063 Extruded Profiles. J. of Materi Eng and Perform 30 (2021) 4691–4699.

[8]. W.D. Finkelnburg, G. Scharf, Some investigations on the metal flow during extrusion of Al alloys, Proceedings of the 5th ET Seminar II (1992) 475–484.

[9]. C. Jowett, J. Adams, C. Daughetee, G. Lea, O.A. Huff, N. Fossl, Scrap allocation, In the Proceedings of the 9th Extrusion Technology Seminar (2008) Florida, USA.

[10]. T. Ishikawa, H. Sano, Y. Yoshida, N. Yukawa, J. Sakamoto, Y. Torzawa, Effect of Extrusion Conditions on Metal Flow and Microstructures of Aluminum Alloys, CIRP Annals 55 (1) (2006) 275-278.

[11]. T. Hatzenbichler, B. Buchmayr, Finite element method simulation of internal defects in billet-to-billet extrusion, Proceedings of the Institution of Mechanical Engineers, Part B: Journal of Engineering Manufacture 224 (2010) 1029-1042.

[12]. S. Lou, Y. Wang, C. Liu, S. Lu, C. Su, Analysis and Prediction of the Billet Butt and Transverse Weld in the Continuous Extrusion Process of a Hollow Aluminum Profile, J. of Mater. Eng. and Perform. 26 (2017) 4121- 4130.

[13]. M. Negozio, R. Pelaccia, L. Donati, B. Reggiani, L. Tomesani, T. Pinter, FEM Validation of front end and back end defects evolution in AA6063 and AA6082 aluminum alloys profiles, Procedia Manufacturing 47 (2020) 202-208, (Cottbus, DE), Elsevier Ltd.

[14]. A. Hensel, T. Spittel, Kraft und Arbeitsbedarf bildsamer Formgeburgsverfahren, 1. Auflage, Leipzig: VEB Deutscher Verlag fur Grundstoffindustrie, 1978.

[15]. M. Schikorra, L. Donati, L. Tomesani, M. Kleiner, The role of friction in the extrusion of AA6060 aluminum alloy, process analysis and monitoring, Journal of Materials Processing Technology 191(1-3) (2007) 288-292.

[16]. A.N. Levanov, Improvement of Metal Forming Processes by means of Useful Effects of Plastic Friction, Journal of Materials Processing Technology 72 (1997) 314-316.

[17]. J. Hallström, Influence of friction on die filling in counterblow hammer forging, J. Mater. Process. Technol. 108 (2000) 21-25.